SCIENTIFIC REPORTS

OPEN

SUBJECT AREAS:
BIOSENSORS
BIOCHEMICAL ASSAYS

Received
29 August 2013

Accepted
3 February 2014

Published
25 February 2014

Correspondence and requests for materials should be addressed to G.X.L. (genxili@nju.edu.cn)

Fabrication of magneto-controlled moveable architecture to develop reusable electrochemical biosensors

Xiaoli Zhu[1], Chang Feng[1], Zonghuang Ye[2], Yangyang Chen[1] & Genxi Li[1,2]

[1]Laboratory of Biosensing Technology, School of Life Sciences, Shanghai University, Shanghai 200444, P. R. China, [2]Department of Biochemistry and State Key Laboratory of Pharmaceutical Biotechnology, Nanjing University, Nanjing 210093, P. R. China.

Electrochemical biosensors have been studied intensively for several decades. Numerous sensing concepts and related interface architectures have been developed. However, all such architectures suffer a trade-off: simple architectures favour usability, whereas complex architectures favour better performance. To overcome this problem, we propose a novel concept by introducing a magneto-controlled moveable architecture (MCMA) instead of the conventional surface-fixed architecture. As a model, human breast cancer cells were used in this study. The results showed that a detection range from 100 to 1 × 10^6 cells could be achieved. Moreover, the whole detection cycle, including the measurement and the regeneration, could be completed in only 2 min. Thus, usability and excellent performance can be achieved in a single biosensor.

Electrochemical biosensors are considered the most promising devices for biological studies and clinical diagnostics[1–4] because of their low cost, ease of use, portability, and simplicity of construction. The detection of various analytes, ranging from ions to cells, has already been achieved with electrochemical biosensors[5–18]. A typical electrochemical biosensor is usually composed of several parts, including a) a sensitive biological element (e.g., enzymes, nucleic acids, antibodies, or tissues, among others) that specifically interacts (binds or recognises) the analyte, b) an interface architecture where the interaction occurs to give rise to a signal picked up by c) a transducer that transforms the signal resulting from the interaction into an electrochemical signal, and d) a reader device that displays the results in a user-friendly way[1,3]. Typically, component b has attracted the most research attention, and the design options are infinite. Thus, researchers have devoted substantial effort to the construction of favourable interface architectures. Numerous strategies have been proposed, and various types of functional materials have been used to construct biosensors; and numerous ingenious interface architectures have been reported[19–36]. However, the construction of many of these ingenious interface architectures is highly complex. Because of the loss of bioactivity of the biological element or damage caused to the architecture during the measurement, the architecture must be reconstructed after it has been used[12–15,33–36]. Unfortunately, tens of minutes or even a few days may be required for the reconstruction, which makes the use of these biosensors inconvenient. In general, simple interfaces provide better usability; however, complex interfaces tend to provide better performance. Some researchers have proposed different strategies to address this usability and performance trade-off, such as the use of disposable screen printed electrodes (SPE) and label-free biosensing[37–41]. However, the greatest obstacle has been the lack of a practical way to regenerate the sensing interface, which has been the bottleneck for the development of different types of electrochemical biosensors, such as immunobiosensors, DNA biosensors, and glucose biosensors, among others.

To overcome this problem, we propose a novel strategy by introducing a magneto-controlled moveable architecture (MCMA). Conventionally, the sensing interface architecture is fixed on the surface of a working electrode; thus, after a component malfunctions, the whole architecture and/or the interface must be reconstructed. In our strategy, the sensing interface is placed on colloidal magnetic nanoparticles (MNPs), which can be easily controlled by a magnetic field, thereby making the interface architecture moveable. Thus, the MCMA in our electrochemical biosensor is dynamically attracted to the surface of the working electrode instead of being fixed on that surface. After a measurement is performed, the electrode can easily be refreshed by attracting the MCMA away from the electrode surface using a magnetic field. Thus, the turnaround time for taking the next measurement is short, thereby enabling the biosensor to perform efficiently and exhibit great usability.

Although MNPs have been previously applied to the fabrication of electrochemical biosensors, they are usually used only as a matrix on the electrodes[42–44] or for separation prior to electrochemical detection[45,46]. This work

represents the first time that magnetic control has been integrated with electrochemical detection and that the interface architecture of an electrochemical biosensor has been made movable under the assistance of MNPs.

Results

In this study, one type of human breast cancer cells (Michigan cancer foundation-7 (MCF-7) cells) was used as a detection model for the biosensor. The principle of the detection is illustrated in Fig. 1. As is illustrated in the scheme, the MCMA includes the detection target (i.e., the MCF-7 cells) and a sensitive biological element (i.e., anti-CEA-antibody-functionalised MNPs (Ab@MNPs) and horseradish-peroxidase-labelled mucin-1 aptamer (HRP-apt)). The anti-CEA antibody and the mucin-1 aptamer here specifically recognise and bind the target cells. The MNPs facilitate magnetic control, and the HRP provides electrochemical catalysis. Thus, the architecture that is usually immobilised on the surface of an electrode is fabricated here in solution and is independent of electrodes. The MCMA can be attracted onto an electrode by placing a magnet under the electrode. Electrochemical signals can be obtained via the sensitive system composed of hydrogen peroxide, thionine, and HRP. To re-generate the electrode, a magnet is placed over the electrode to remove the MCMA. Therefore, cycling of the detection and regeneration is very convenient through magnetic control. The primary difference between this biosensor and conventional electrochemical biosensors is the use of the MCMA; thus, the corresponding sensing interface can be very simple and user-friendly.

We also performed experiments to optimise the conditions used to prepare the MCMA. Details concerning the synthesis and characterisation of Ab@MNPs and HRP-apt are provided in the Supplementary Methods section (Figs. S1 and S2). An effective MCMA was obtained by incubating MCF-7 cells with the Ab@MNPs and the HRP-apt. Free Ab@MNPs and HRP-apt were then washed out of the solution using low-speed centrifugation, and magnetic separation was used to remove free MCF-7 cells. Thus, the MCMAs were constructed, and were dispersed in the test solution, which could be controlled by a magnetic field.

Because the electrode-electrolyte sensing interface was simple and user-friendly, no functional design was required. Two basic preconditions should be satisfied. First, the interface should be able to facilitate enzyme-assisted electrochemical signals. We examined these signals by studying the electrochemical response of different electrode-electrolyte interfaces. A tail with different chemical groups added to the gold electrode was adopted to generate the interface with an aqueous electrolyte (phosphate buffer solution, 10 mM, pH 7.4). As shown in Fig. 2, the corresponding cyclic voltammetric response was obtained for all cases after the sequential addition of the substrate, electron mediator, and enzyme (hydrogen peroxide, thionine, and HRP, respectively) to the electrolyte. When HRP was added as the last step, an apparent peak current with a shape of a catalytic wave was obtained (blue curves), which suggested that the HRP-catalysed and thionine-mediated electrochemical reduction of hydrogen peroxide occurred. Although hydrogen peroxide and thionine also exhibited a direct electrochemical response, the efficiency of electron transfer was much lower than that with the enzyme HRP. The electrochemical catalytic process can be described by Equations (1)–(4):

$$\mathrm{HRP}\left(\mathrm{Fe^{III}}\right)+\mathrm{H_2O_2}\rightarrow\text{compound I}+\mathrm{H_2O} \quad (1)$$

$$\text{compound I}+\text{thionine(Red)}\rightarrow\text{compound II}+\text{thionine(Ox)}^{*} \quad (2)$$

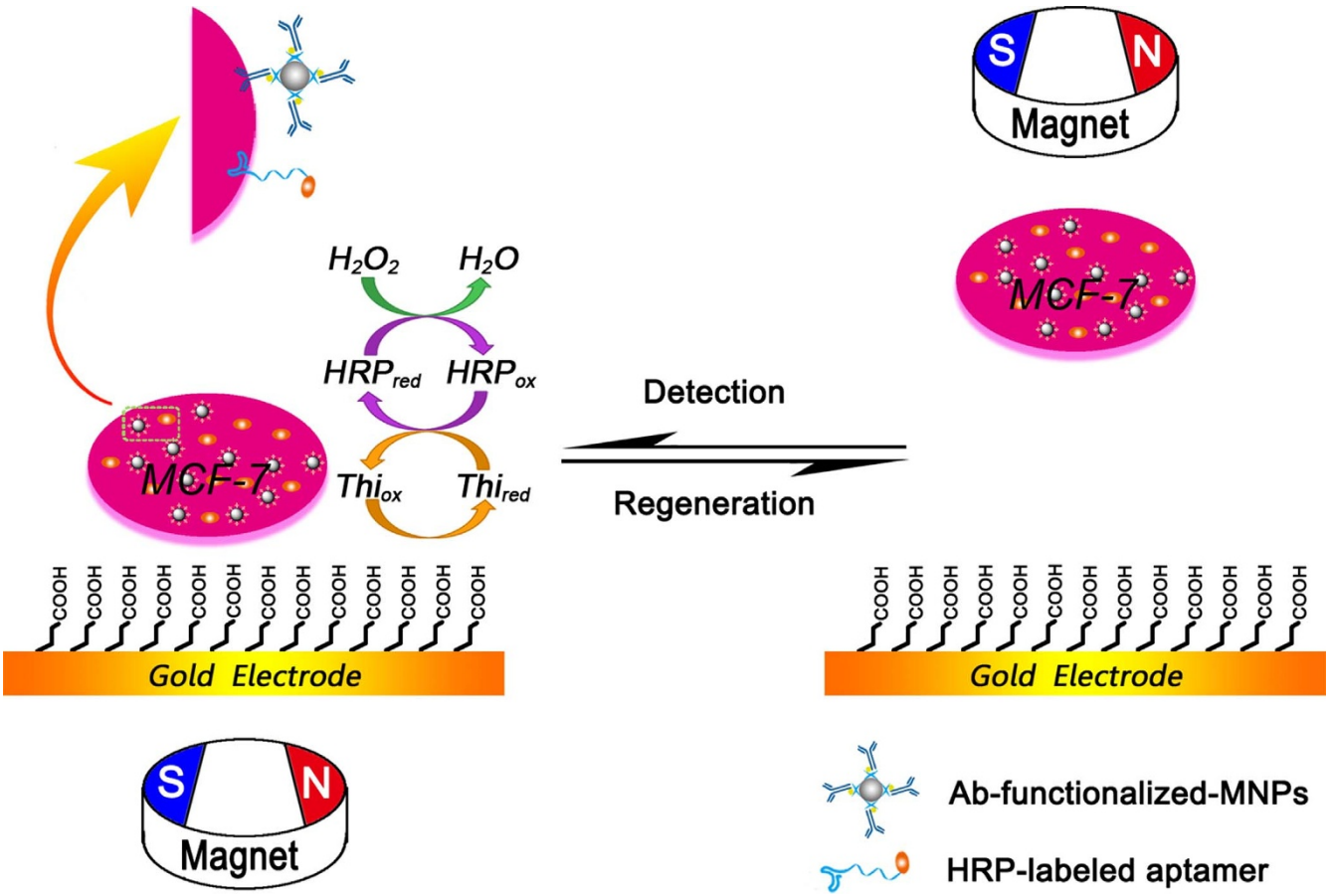

Figure 1 | Schematic illustration of the MCMA-based reusable electrochemical biosensor for the detection of human breast cancer cells.

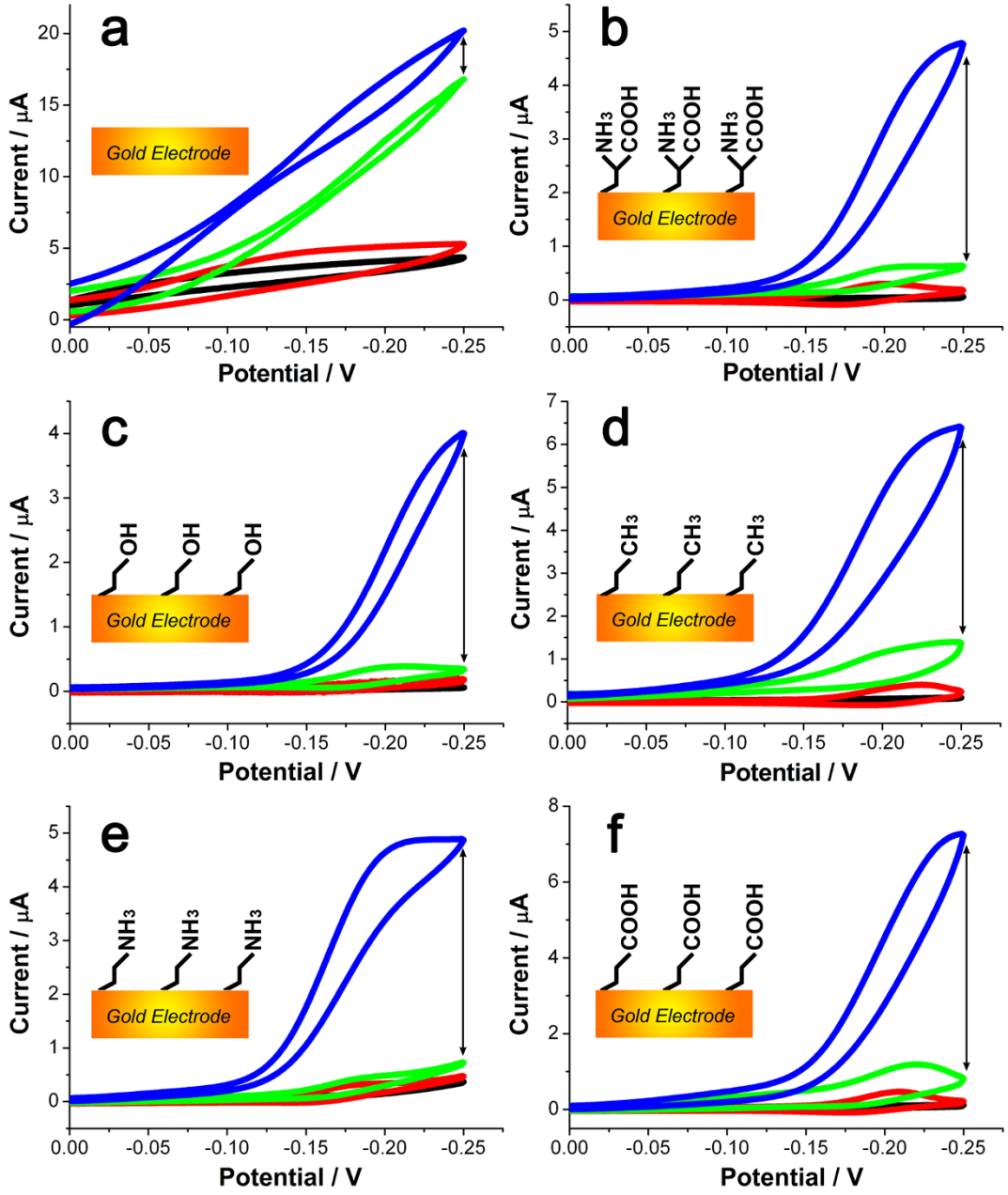

Figure 2 | Cyclic voltammetric response of different chemical-group-tailed gold electrodes in a PBS electrolyte (10 mM, pH 7.4) (black curves) after the sequential addition of hydrogen peroxide (red curves), thionine (green curves), and HRP (blue curves). From (a) to (f): bare gold electrode, gold electrode modified with cysteine, ethanethiol, mercaptohexanol, mercaptoethylamine, and mercaptoacetic acid, respectively.

$$\text{compound II} + \text{thionine(Ox)}^{*} \rightarrow \text{HRP}\left(\text{Fe}^{\text{III}}\right) + \text{thionine(Ox)} \quad (3)$$

$$\text{thionine(Ox)} + 2e^{-} + 2H^{+} \rightarrow \text{thionine(Red)} \quad (4)$$

where "Ox" indicates the oxidative states and "Red" indicates the reductive states. The electrochemical workstation provided two electrons in Equation (4), representing the catalytic wave. The change in the current (indicated by double-sided arrows in Fig. 2) can be regarded as the effective readout signal, which was significant in all of the examined cases except the bare gold electrode[47–49]. With the exception of the bare gold electrode, the other five chemically modified electrodes all satisfied the signal readout requirement. The interface also requires self-cleaning properties because the physical adsorption of the MCMA onto the electrode is unwanted. We conducted experiments in which we compared the adsorption of the target MCF-7 cells on the five chemically modified electrodes. The results showed that cells on the methyl- and carboxyl-tailed electrodes were more easily washed away (Fig. 3), which can be ascribed to the repulsion of the polar molecules on the cells with the hydrophobic methyl-tailed surface or to the electrostatic repulsion between negatively charged cells and the carboxyl-tailed surface. Thus, both the methyl- and carboxyl-tailed electrodes were favourable. Because ethanethiol (methyl-tailed) is more volatile and toxic, mercaptoacetic acid (carboxyl-tailed) was used for the construction of the electrode-electrolyte sensing interface.

We assembled the biosensing device and conducted electrochemical measurements of MCF-7 cells. Fig. 4 displays photographs of the biosensing device. The carboxyl-tailed gold electrode, which functioned as the working electrode, was positioned face-up to favour magnetic control. A saturated calomel reference electrode and a platinum counter electrode were also used to complete the three-electrode system. The MCMA, the substrate, and the electron mediator were added directly to the test solution (10 mM phosphate buffer solution,

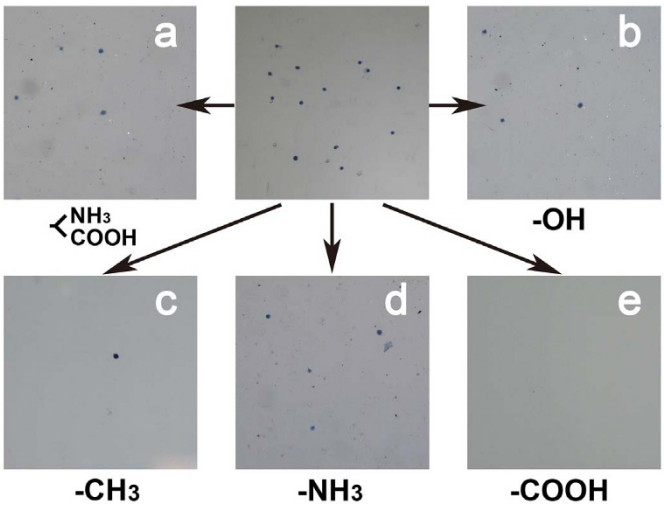

Figure 3 | Microscopic observation of cells on different chemical-group-tailed gold-sputtered cover glass. Top centre: before being rinsed; others: rinsed after adsorption for 5 min. From (a) to (e): gold electrode modified with cysteine, ethanethiol, mercaptohexanol, mercaptoethylamine, and mercaptoacetic acid, respectively. The gold-sputtered cover glass was prepared using an ion sputter coater.

pH 7.4). When a magnet was placed under the working electrode, the MCMA was attracted to the surface of the working electrode. After only 30 s, the MCMA assembled on the surface of the working electrode and was visible to the naked eyes. Cyclic voltammetric measurements were then conducted, as shown in Fig. 5a, and a typical catalytic wave was obtained (cyan curve). In the control experiments, the absence of either Ab@MNPs (black and red curves) or HRP-apt (blue and green curves) resulted in low peak currents. Because the MCF-7 cells attract the Ab@MNPs and the HRP-apt to compose the MCMA, the signal intensity was dependant on the quantity of MCF-7 cells. Thus, an increase in current response was observed when the quantity of MCF-7 cells was increased (Fig. 5b). Fig. 5c shows the relationship between the peak current and the cell number. The current exhibited a linear relationship with the logarithm of the cell number in the range from 100 to 1×10^6 cells; the linear equation was $Y = 1.087 + 0.788X$ ($R = 0.994$). The relative standard deviations (RSDs) of the data points ranged from 2.4%–5.2% ($n = 4$). Therefore, the favourable detection of MCF-7 cells with a large detection range and a good detection limit can be achieved with this biosensor.

To regenerate the biosensor, the magnetic field was placed above the working electrode. After being washed with water, the working electrode was immediately regenerated and exhibited a golden, mirror-like appearance; this change showed that the electrode was ready for the next test. The current response for the measurement of 1×10^6 cells in three cycles is shown in Fig. 5d. The RSDs of the data points ranged from 2.5%–5.9% ($n = 4$). Thus, continual tests at intervals less than 2 min can be successfully achieved. It is noted that a little passivation still exists, representing the slight increase of the background current. This is owing to the inevitable slight adsorption of the MCMA on the surface of the working electrode after the gentle rinsing. Nevertheless, a better treatment of the working electrode (e.g., ultrasonication in water for another 2 min) was proven to remove the passivation (Supplementary Fig. S3a). The stability of the biosensor was also tested by placing the electrode in dark for 7 days, and no passivation was observed (Supplementary Fig. S3b).

Discussion

In summary, we have proposed a novel strategy in which MCMA is adopted for the fabrication of reusable electrochemical biosensors that exhibit excellent performance and practical usability. MCF-7 cells that were used as a model were successfully detected. In addition

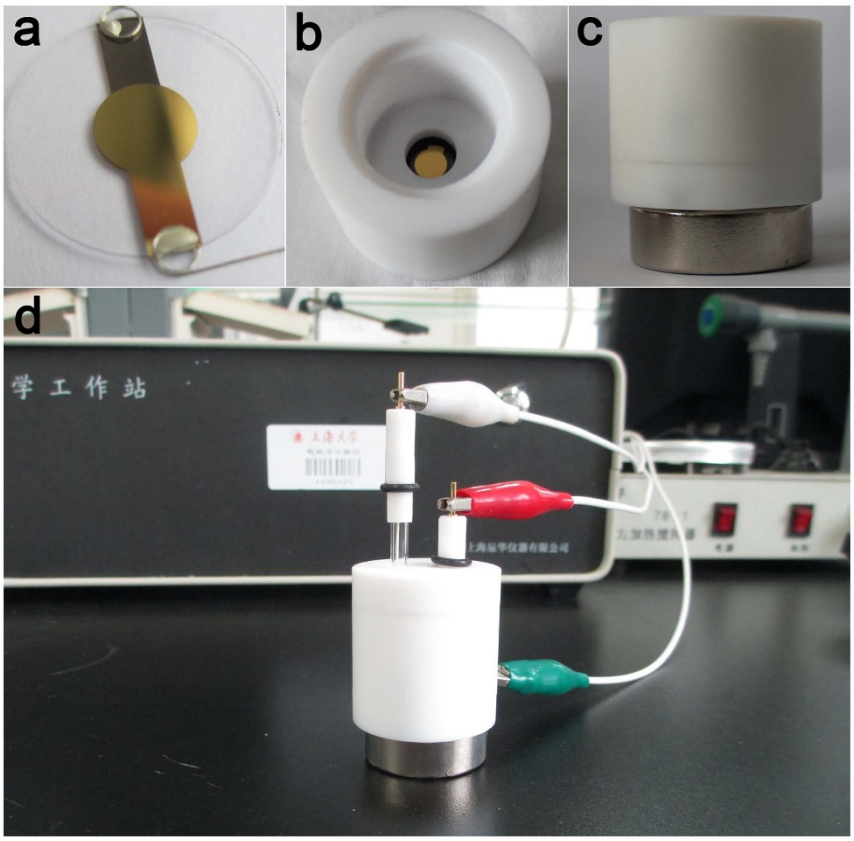

Figure 4 | Photographs of the device: (a) the gold-wafer electrode; (b) the electrolytic cell; (c) a magnet placed under the gold electrode; and (d) the overall appearance of the three-electrode system.

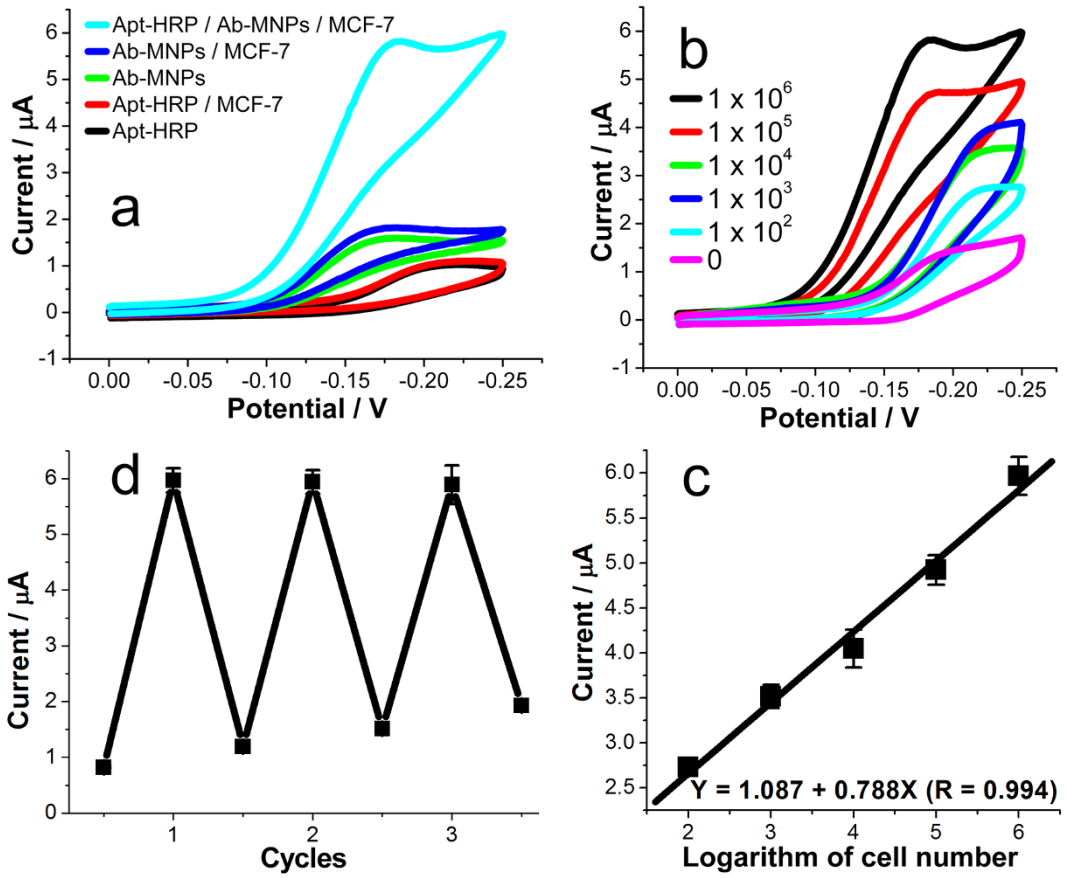

Figure 5 | Cyclic voltammetric responses of (a) the complete (cyan curve) or incomplete (black, red, green, and blue curves) MCMA in the electrolyte containing 20 μM thionine and 6 mM H_2O_2 and (b) the MCMA fabricated with different amounts of cells. Other conditions were the same as those in (a). (c) The relationship between the peak current and the cell numbers. The dots represent the currents of the corresponding cyclic voltammogram at −0.25 V. (d) The current response for the MCMA with 1×10^6 cells over three cycles. The top dots represent responsive currents, whereas the bottom dots represent background currents. All dots were taken from the corresponding cyclic voltammogram at −0.25 V.

to its favourable performance and practical usability, the novel biosensor may also exhibit other advantages over traditional biosensors: a) the MCMA can be constructed in batches, which may contribute to high-throughput measurements; b) dual-recognition or even multi-recognition can be introduced simultaneously to the detection target, thereby substantially shortening the detection time; and c) the biosensor can be regenerated very easily and rapidly; thus, detection in sequence can be achieved on a single electrode without waiting for further treatment of the samples and the electrode. In addition, opportunities exist to further develop this novel biosensor using other strategies, such as a) the construction of a self-cleaning electrode surface via the adoption of superhydrophobic materials to facilitate control of a universal MCMA; b) the inclusion of different architectures in the MCMA, with numerous possibilities for the detection of different targets; c) the use of previously reported strategies to achieve better performance of a biosensor, e.g., enzyme-assisted signal amplification, can be adapted to the MCMA. Thus, the strategy proposed in this study to construct reusable electrochemical biosensors could be employed for the rapid development of different types of biosensors in the near future.

Methods

Preparation of the magneto-controlled moveable architecture (Ab@MNPs/cell/HRP-apt). The detailed methods for the cell culture and the synthesis of Ab@MNPs and HRP-apt can be found in the Supplementary Methods section. In total, 100 μL of Ab@MNPs, 100 μL of cell suspension, and 10 μL of HRP-apt were mixed together and incubated at room temperature for 1 h. The Ab@MNPs/cell/HRP-apt MCMA was subsequently separated under a magnetic field and washed twice in phosphate-buffered saline (PBS) (10 mM, pH 7.4). The Ab@MNPs/cell/HRP-apt MCMA was prepared after it was magnetically separated and redispersed in 300 μL of PBS.

Preparation of the chemical group-tailed gold electrode. A polished gold wafer electrode obtained from CHI Instruments (Shanghai, China) was first immersed in piranha solution (H_2SO_4/H_2O_2, 7 : 3, v/v) for 5 min, followed by rinsing with copious amounts of double-distilled water. (Caution: Piranha solution reacts violently with organic solvents and should be handled with great care.) The electrode was subsequently cleaned electrochemically in 0.5 M H_2SO_4 by potential scanning between 0 and 1.6 V until a reproducible cyclic voltammogram was obtained. Finally, the electrode was washed with double-distilled water and dried in a gentle stream of high-purity nitrogen. The clean gold electrode was immersed in 200 μL of 10 mM mercaptoacetic acid and was stored in the dark at 4°C for 16 h. The same procedure was used for the modification of mercaptoethylamine, ethanethiol, mercaptohexanol, and cysteine.

Electrochemical measurements. The electrochemical measurements were performed on a model 660C electrochemical analyser (CH Instruments). A conventional three-electrode system consisting of the gold electrode, a saturated calomel reference electrode, and a platinum counter electrode was used for all of the electrochemical measurements. The device is shown in Fig. 4. A PBS solution (5 mL, 10 mM, pH 7.4) containing 20 μM thionine and 6 mM H_2O_2 was used as the electrolyte. Before the measurements were performed, the MCMA was directly added to the electrolyte with a microinjector. A magnet was placed under the electrode for 30 s to attract the MCMA onto the working electrode. Cyclic voltammetric measurements were then performed in the potential range of 0 ~ −0.25 V at a scan rate of 5 mV/s while the magnet was kept still. To regenerate the electrode after the cyclic voltammetric measurements, the magnet was placed over the working electrode for 30 s. After being further rinsed with double-distilled water, the electrode was ready for another test. All of the electrochemical measurements were repeated at least four times, and the data points presented represent averages from at least four independent experiments.

1. Ronkainen, N. J., Halsall, H. B. & Heineman, W. R. Electrochemical biosensors. *Chem. Soc. Rev.* **39**, 1747–1763 (2010).

2. Wang, J. *Analytical Electrochemistry*, Edn. 3rd. (Wiley-VCH, Hoboken, New Jersey, USA, 2006).
3. Grieshaber, D., MacKenzie, R., Vörös, J. & Reimhult, E. Electrochemical biosensors - Sensor principles and architectures. *Sensors* **8**, 1400–1458 (2008).
4. Pohanka, M. & Skladai, P. Electrochemical biosensors - principles and applications. *J. Appl. Biomed.* **6**, 57–64 (2008).
5. Das, J. *et al*. An ultrasensitive universal detector based on neutralizer displacement. *Nat. Chem.* **4**, 642–648 (2012).
6. Shirazi, S. & Davies, I. R. Electrochemical detection of nitrite and nitrate using a microreductor chamber. *Nature* 6–6 (1998).
7. Heller, A. & Feldman, B. Electrochemical glucose sensors and their applications in diabetes management. *Chem. Rev.* **108**, 2482–2505 (2008).
8. Hashemi, P. *et al*. Brain dopamine and serotonin differ in regulation and its consequences. *Proc. Natl. Acad. Sci. U.S.A.* **109**, 11510–11515 (2012).
9. Liu, X. H. *et al*. Real-time mapping of a hydrogen peroxide concentration profile across a polymicrobial bacterial biofilm using scanning electrochemical microscopy. *Proc. Natl. Acad. Sci. U.S.A.* **108**, 2668–2673 (2011).
10. Wang, Y. X. *et al*. Nanoelectrodes for determination of reactive oxygen and nitrogen species inside murine macrophages. *Proc. Natl. Acad. Sci. U.S.A.* **109**, 11534–11539 (2012).
11. Drummond, T. G., Hill, M. G. & Barton, J. K. Electrochemical DNA sensors. *Nat. Biotechnol.* **21**, 1192–1199 (2003).
12. Pheeney, C. G., Guerra, L. F. & Barton, J. K. DNA sensing by electrocatalysis with hemoglobin. *Proc. Natl. Acad. Sci. U.S.A.* **109**, 11528–11533 (2012).
13. Wen, Y. L. *et al*. DNA nanostructure-based interfacial engineering for PCR-free ultrasensitive electrochemical analysis of microRNA. *Sci. Rep.* **2**, 867; doi:10.1038/srep00867 (2012).
14. Xiao, Y., Lubin, A. A., Baker, B. R., Plaxco, K. W. & Heeger, A. J. Single-step electronic detection of femtomolar DNA by target-induced strand displacement in an electrode-bound duplex. *Proc. Natl. Acad. Sci. U.S.A.* **103**, 16677–16680 (2006).
15. Cai, D. *et al*. A molecular-imprint nanosensor for ultrasensitive detection of proteins. *Nat. Nanotechnol.* **5**, 597–601 (2010).
16. Li, G. X. & Miao, P. *Electrochemical Analysis of Proteins and Cells*. (Springer, Berlin, Germany, 2012).
17. Doerr, A. Imaging impedance. *Nat. Methods* **8**, 202 (2011).
18. Arya, S. K. & Bhansali, S. Lung cancer and its early detection using biomarker-based biosensors. *Chem. Rev.* **111**, 6783–6809 (2011).
19. Li, G. X. in Nanotechnologies for Life Sciences, Vol. 8. (ed. C. Kumar) 278–310 (Wiley-VCH, New York, USA, 2007).
20. Suginta, W., Khunkaewla, P. & Schulte, A. Electrochemical biosensor applications of polysaccharides chitin and chitosan. *Chem. Rev.* **113**, 5458–5479 (2013).
21. Chen, A. & Chatterjee, S. Nanomaterials based electrochemical sensors for biomedical applications. *Chem. Soc. Rev.* **42**, 5425–5438 (2013).
22. Song, S. P. *et al*. Functional nanoprobes for ultrasensitive detection of biomolecules. *Chem. Soc. Rev.* **39**, 4234–4243 (2010).
23. Tamayo, J., Kosaka, P. M., Ruz, J. J., San Paulo, A. & Calleja, M. Biosensors based on nanomechanical systems. *Chem. Soc. Rev.* **42**, 1287–1311 (2013).
24. Willner, I. & Zayats, M. Electronic aptamer-based sensors. *Angew. Chem. Int. Ed.* **46**, 6408–6418 (2007).
25. Walcarius, A. Mesoporous materials and electrochemistry. *Chem. Soc. Rev.* **42**, 4098–4140 (2013).
26. Li, G. X. in Encyclopedia of Sensors, Vol. 8. (eds. Grimes, C. A., Dickey, E. C. & Pishko, M. V.) 301–313 (American Scientific Publishers, Stevenson Ranch, USA, 2006).
27. Zhou, M. & Dong, S. Bioelectrochemical interface engineering: toward the fabrication of electrochemical biosensors, biofuel cells, and self-powered logic biosensors. *Acc. Chem. Res.* **44**, 1232–1243 (2011).
28. Lubin, A. A. & Plaxco, K. W. Folding-based electrochemical biosensors: the case for responsive nucleic acid architectures. *Acc. Chem. Res.* **43**, 496–505 (2010).
29. Liu, Y., Dong, X. & Chen, P. Biological and chemical sensors based on graphene materials. *Chem. Soc. Rev.* **41**, 2283–2307 (2012).
30. Famulok, M. & Mayer, G. Aptamer modules as sensors and detectors. *Acc. Chem. Res.* **44**, 1349–1358 (2011).
31. Wu, Y., Wei, W. & Liu, S. Target-triggered polymerization for biosensing. *Acc. Chem. Res.* **45**, 1441–1450 (2012).
32. Lang, X. Y. *et al*. Nanoporous gold supported cobalt oxide microelectrodes as high-performance electrochemical biosensors. *Nat. Commun.* **4**, 2169 (2013).
33. Zhu, X., Han, K. & Li, G. Magnetic nanoparticles applied in electrochemical detection of controllable DNA hybridization. *Anal. Chem.* **78**, 2447–2449 (2006).
34. Mani, V., Chikkaveeraiah, B. V., Patel, V., Gutkind, J. S. & Rusling, J. F. Ultrasensitive immunosensor for cancer biomarker proteins using gold nanoparticle film electrodes and multienzyme-particle amplification. *ACS Nano* **3**, 585–594 (2009).
35. Sharma, P. *et al*. Enhancing electrochemical detection on graphene oxide-CNT nanostructured electrodes using magneto-nanobioprobes. *Sci. Rep.* **2**, 877; doi:10.1038/srep00877 (2012).
36. Cheng, W., Ding, L., Ding, S. J., Yin, Y. B. & Ju, H. X. A simple electrochemical cytosensor array for dynamic analysis of carcinoma cell surface glycans. *Angew. Chem. Int. Ed.* **48**, 6465–6468 (2009).
37. Metters, J. P., Kadara, R. O. & Banks, C. E. New directions in screen printed electroanalytical sensors: an overview of recent developments. *Analyst* **136**, 1067–1076 (2011).
38. Renedo, O. D., Alonso-Lomillo, M. A. & Martinez, M. J. Recent developments in the field of screen-printed electrodes and their related applications. *Talanta* **73**, 202–219 (2007).
39. Hunt, H. K. & Armani, A. M. Label-free biological and chemical sensors. *Nanoscale* **2**, 1544–1559 (2010).
40. Du, Y., Li, B. & Wang, E. "Fitting" makes "sensing" simple: label-free detection strategies based on nucleic acid aptamers. *Acc. Chem. Res.* **46**, 203–213 (2013).
41. Luo, X. & Davis, J. J. Electrical biosensors and the label free detection of protein disease biomarkers. *Chem. Soc. Rev.* **42**, 5944–5962 (2013).
42. Zhang, Y. X. *et al*. Electrochemical sensor for bisphenol A based on magnetic nanoparticles decorated reduced graphene oxide. *Talanta* **107**, 211–218 (2013).
43. Li, X. C. *et al*. Magnetic titania-silica composite–Polypyrrole core–shell spheres and their high sensitivity toward hydrogen peroxide as electrochemical sensor. *J. Colloid Interf. Sci.* **387**, 39–46 (2012).
44. Tang, D., Yuan, R. & Chai, Y. Ultrasensitive electrochemical immunosensor for clinical immunoassay using thionine-doped magnetic gold nanospheres as labels and horseradish peroxidase as enhancer. *Anal. Chem.* **80**, 1582–1588 (2008).
45. Karadeniz, H., Erdem, A., Kuralay, F. & Jelen, F. Indicator-based and indicator-free magnetic assays connected with disposable electrochemical nucleic acid sensor system. *Talanta* **78**, 187–192 (2009).
46. Luo, X. T., Xu, J. J., Barford, J. & Hsing, I. M. Magnetic particle based electrochemical sensing platform for PCR amplicon detection. *Electrochem. Commun.* **12**, 531–534 (2010).
47. Zeis, R., Lei, T., Sieradzki, K., Snyder, J. & Erlebacher, J. Catalytic reduction of oxygen and hydrogen peroxide by nanoporous gold. *J. Catal.* **253**, 132–138 (2008).
48. Jv, Y., Li, B. X. & Cao, R. Positively-charged gold nanoparticles as peroxidiase mimic and their application in hydrogen peroxide and glucose detection. *Chem. Commun.* **46**, 8017–8019 (2010).
49. Wang, S. *et al*. Comparison of the peroxidase-like activity of unmodified, amino-modified, and citrate-capped gold nanoparticles. *ChemPhysChem* **13**, 1199–1204 (2012).

Acknowledgments

This work was supported by the National Science Fund for Distinguished Young Scholars (Grant No. 20925520), the National Natural Science Foundation of China (Grant Nos. 61001035, 21235003), the "Chen Guang" project of the Shanghai Municipal Education Commission and the Shanghai Education Development Foundation (No. 10CG42), the Innovation Program of Shanghai Municipal Education Commission (No. 12YZ004), and the Shanghai Science and Technology Committee (Grant No. 11DZ2272100).

Author contributions

X.Z. and G.L. designed the experiments and the methods; C.F. and Z.Y. performed the experiments; Y.C. cultured the cells; X.Z., C.F., Z.Y. and Y.C. jointly analysed the data; X.Z. and G.L. wrote the manuscript.

Additional information

Supplementary information accompanies this paper at http://www.nature.com/scientificreports

Competing financial interests: The authors declare no competing financial interests.

How to cite this article: Zhu, X.L., Feng, C., Ye, Z.H., Chen, Y.Y. & Li, G.X. Fabrication of magneto-controlled moveable architecture to develop reusable electrochemical biosensors. *Sci. Rep.* **4**, 4169; DOI:10.1038/srep04169 (2014).